



23 **Abstract**

24 **Purpose:** *Pseudomonas aeruginosa* keratitis is a severe ocular infection that can lead  
25 to perforation of the cornea. In this study we evaluated the role of bacterial quorum  
26 sensing in generating corneal perforation and bacterial proliferation and tested whether  
27 co-injection of the predatory bacteria *Bdellovibrio bacteriovorus* could alter the clinical  
28 outcome. *P. aeruginosa* with *lasR* mutations were observed among keratitis isolates  
29 from a study collecting samples from India, so an isogenic *lasR* mutant strain of *P.*  
30 *aeruginosa* was included.

31 **Methods:** Rabbit corneas were intracorneally infected with *P. aeruginosa* strain PA14 or  
32 an isogenic  $\Delta$ *lasR* mutant and co-injected with PBS or *B. bacteriovorus*. After 24 h, eyes  
33 were evaluated for clinical signs of infection. Samples were analyzed by scanning  
34 electron microscopy, optical coherence tomography, sectioned for histology, and  
35 corneas were homogenized for CFU enumeration and for inflammatory cytokines.

36 **Results:** We observed that 54% of corneas infected by wild-type PA14 presented with a  
37 corneal perforation (n=24), whereas only 4% of PA14 infected corneas that were co-  
38 infected with *B. bacteriovorus* perforate (n=25). Wild-type *P. aeruginosa* proliferation was  
39 reduced 7-fold in the predatory bacteria treated eyes. The  $\Delta$ *lasR* mutant was less able to  
40 proliferate compared to the wild-type, but was largely unaffected by *B. bacteriovorus*.

41 **Conclusion:** These studies indicate a role for bacterial quorum sensing in the ability  
42 of *P. aeruginosa* to proliferate and cause perforation of the rabbit cornea. Additionally,  
43 this study suggests that predatory bacteria can reduce the virulence of *P. aeruginosa* in  
44 an ocular prophylaxis model.

45

## 46 1. Introduction

47 Predatory bacteria, such as *Bdellovibrio bacteriovorus*, have been suggested as an  
48 alternative approach for treatment antibiotic resistant bacterial infections in general [1-6].  
49 *B. bacteriovorus* is a Gram-negative bacterium that is an obligate predator of other  
50 Gram-negative bacteria. Given the preponderance of Gram-negative bacteria in causing  
51 contact-lens related keratitis, predatory bacteria have been hypothesized as treatments  
52 for eye infections [7-9], and are largely non-toxic and non-inflammatory when applied in  
53 great numbers to a corneal epithelial cell line and intact and wounded ocular surfaces [7,  
54 10]. These have been tested to prevent bacterial proliferation on the ocular surface with  
55 some success and to prevent the development of keratitis in a mouse model using  
56 *Escherichia coli* as a pathogen [11, 12].

57 Unlike *E. coli*, *Pseudomonas aeruginosa* is the leading cause of contact lens  
58 associated keratitis, a blinding infection [13-15]. Antibiotic resistant *P. aeruginosa*  
59 keratitis isolates are associated with worse clinical outcomes [16-19]. Previous work  
60 showed that *B. bacteriovorus* predation is not influenced by antibiotic resistance status  
61 of its prey [3, 5, 7] and is even effective at clearing antibiotic tolerant biofilms [20, 21]. A  
62 recent study showed that around 20% of *P. aeruginosa* keratitis isolates isolated in India  
63 from 2006-2010 had mutations in the *lasR* gene and that these strains were correlated  
64 with worse visual outcomes in patients [22]. The LasR protein is a major regulator of  
65 quorum sensing and important in regulation of numerous virulence-associated genes  
66 [23].

67 In this study we evaluated whether *B. bacteriovorus* strain HD100 could act as a  
68 “living antibiotic” in a rabbit keratitis infection model using a clade 2 (cytotoxic/ExoU<sup>+</sup>)  
69 and highly virulent *P. aeruginosa* strain. This was a proof-of-concept prevention model  
70 rather than a treatment model. The study found that the predatory bacteria caused mild-

71 moderate inflammation, but were able to reduce *P. aeruginosa* proliferation and most  
72 importantly significantly reduced the frequency of corneal perforation events caused by  
73 *P. aeruginosa*. We also observed that an isogenic *P. aeruginosa*  $\Delta lasR$  mutant was  
74 unable to replicate in the rabbit cornea and caused significantly fewer corneal  
75 perforations, but was not significantly reduced by *B. bacteriovorus* in the cornea.

76

## 77 **2. Methods**

### 78 **2.1. Bacterial strains and culture**

79 *B. bacteriovorus* HD100 (ATCC 15356) [24] was used for this study. Preparation of *B.*  
80 *bacteriovorus* followed prior reports [10, 12] where *B. bacteriovorus* was incubated with  
81  $\sim 10^9$  CFU/ml *E. coli* diaminopimelic acid auxotroph strain WM3064 for 24 h at 30°C. The  
82 resulting mixture was passed multiple times through a 0.45- $\mu$ m Millex<sup>®</sup>-HV pore-size  
83 filter (Millipore, Billerica, MA, USA) to remove remaining prey. Predators were washed  
84 with phosphate buffered saline (PBS) and concentrated centrifugation. *B. bacteriovorus*  
85 was suspended in PBS to  $1.5 \times 10^{10}$  PFU/ml *B. bacteriovorus*.

86 For a pathogen, the cytotoxic (ExoU+) / clade II strain UCBPP-PA14 (PA14) [25-  
87 28] and an isogenic  $\Delta lasR$  mutant were used [29]. These were inoculated from single  
88 colonies into LB medium and grown with aeration at 30°C or 37°C. For inoculation, *P.*  
89 *aeruginosa* were diluted in phosphate buffered saline (PBS) to achieve the inoculum  
90 ( $\sim 2-4 \times 10^3$  CFU in 10  $\mu$ l).

91

### 92 **2.2. Bacterial keratitis studies**

93 The experiments in this study conformed to the ARVO Statement on the Use of Animals  
94 in Ophthalmic and Vision Research and were approved by the University of Pittsburgh's  
95 Institutional Animal Care and Use Committee (IACUC Protocols 15025331 and  
96 18022194).

97 Female New Zealand White rabbits (1.1-1.4 kg) were obtained from the  
98 Oakwood Research Facility through Charles River Laboratories. The rabbits were  
99 anesthetized with 40 mg/kg of ketamine and 4 mg/kg of xylazine administered  
100 intramuscularly. The corneas of the right eyes only were anesthetized with topical 0.5%  
101 proparacaine and injected intrastromally with the 10  $\mu$ l of *P. aeruginosa* (~2000 CFU) in  
102 PBS or PBS alone as a control. Actual inocula for each trial was determined using the  
103 EddyJet 2 spiral plating system (Neutec Group Inc., Farmingdale, NY) on 5% trypticase  
104 soy agar with 5% sheep's blood plates. Plates were incubated for ~18-20 h at 37°C and  
105 the colonies were enumerated (Flash and Grow colony counting system, Neutec Group,  
106 Inc). This was followed by a 25  $\mu$ l injection of *B. bacteriovorus* in PBS (~4x10<sup>8</sup>) or PBS.

107 At 24 h post-injection, the eyes were evaluated for ocular signs of inflammation  
108 using a slit-lamp according to a modified McDonald-Shaddock grading system [30].  
109 Rabbits were systemically anesthetized with ketamine and xylazine as described above  
110 and euthanized with Euthasol solution following the 2020 AVMA Euthanasia Guidelines.

111 Corneal buttons were harvested using a 10 mm trephine and placed into Lysing  
112 Matrix A tubes (MP Biomedicals) containing 1 ml of PBS. The corneas were then  
113 homogenized with an MP Fast Prep-24 homogenizer (MP Biomedicals), and the  
114 numbers of corneal bacteria were enumerated as described above. The centrifuged and  
115 filtered homogenate (Millipore 0.22 $\mu$ m PVDF filter) was frozen for ELISA analysis (IL-1 $\beta$   
116 kit (Sigma-Aldrich RAB1108). MMP9 ELISA) following the manufacturer's guidelines.  
117 Additional corneas were fixed with paraformaldehyde (4%) in PBS, embedded in  
118 paraffin, and 5  $\mu$ m sections were stained with hematoxylin and eosin. Sections were  
119 viewed using an Olympus Provis AX-70 microscope and images captured with  
120 MagnaFire 2.1 software.

121 In another set of animals, the whole eyes were removed following euthanasia  
122 and stored individually in 25 mm of PBS and kept on ice. Within one hour, their corneas

123 were scanned by optical coherence tomography (OCT) using a Bioptigen Envisu R2210  
124 system with InVivoVue software (Leica Microsystems) following the same general  
125 approach described elsewhere [31]. Briefly, the system was modified with a broadband  
126 superluminescent diode (Superlum, Dublin, Ireland  $\lambda = 870$  nm,  $\Delta\lambda = 200$  nm, 20,000 A-  
127 scans/second). OCT volume scans of the central cornea were acquired using a 10mm  
128 telecentric lens for anterior segment imaging and a scan pattern: 6mm x 6mm x 2mm  
129 (1000 x 100 x 1024 pixel sampling), with 1 Frame per B-scans, i.e. no repetitions. At  
130 least three scans were obtained of each sample and the best quality scan chosen for  
131 analysis. The most common issue was a high signal at the cornea apex that reduced  
132 visibility directly underneath. Scans of a given eye were completed in less than six  
133 minutes. The B-scans were loaded into Fiji for visualization as image volumes and to  
134 export stills and movies [32].

135

### 136 **2.3. Scanning Electron Microscopy**

137 Electron microscopy was performed as previously described [12]. Rabbit corneal buttons  
138 were fixed with glutaraldehyde (3%) at room temperature for 24h and washed with PBS.  
139 Samples were pinned to prevent curling and post-fixed using osmium tetroxide (1%),  
140 dehydrated with ethanol (30–100%), immersed in hexamethyldisilazane and air-dried.  
141 Samples were mounted to aluminum stubs and sputter coated with gold/palladium (6  
142 nm). Scanning electron microscopy was performed using a JEOL JSM-6335F scanning  
143 electron microscope (3 kV).

144

### 145 **2.4. In vitro predation assay**

146 *P. aeruginosa* were grown at 37°C in LB broth on a tissue culture rotor, centrifuged and  
147 suspended in HEPES buffer (25 mM HEPES with 3 mM MgCl<sub>2</sub> and 2 mM CaCl<sub>2</sub>).

148 Aliquots of *P. aeruginosa* (0.5 ml,  $\sim 1 \times 10^9$  CFU) and *B. bacteriovorus* (0.5 ml,  $\sim 2 \times 10^8$

149 PFU) and 4 ml of HEPES buffer were added to 15 ml conical polypropylene tubes and  
150 incubated at 30°C. At 24 h bacteria were serially diluted and plated on LB agar plates to  
151 determine surviving *P. aeruginosa*. Log reductions were calculated as compared to a  
152 predator free control survival at the same time point.

153

## 154 **2.5. Statistical analysis**

155 Kruskal-Wallis with Dunn's post-test was used for non-parametric analysis and ANOVA  
156 with Tukey's post-test or Student's T-tests for parametric analysis. Contingency analysis  
157 was performed with Chi-Square test followed by Fisher's Exact test for pair-wise  
158 comparisons. All analyses were done with GraphPad Prism software.

159

## 160 **3. Results**

### 161 **3.1. Evaluation of the antimicrobial efficacy of *B. bacteriovorus* in a *P. aeruginosa*** 162 **keratitis model.**

163 The ability of the predatory bacteria *B. bacteriovorus* strain HD100 to prevent *P.*  
164 *aeruginosa* proliferation in a bacterial keratitis model was evaluated. *P. aeruginosa* was  
165 used because it is a major cause of corneal infection. In this study either 10 µl of *P.*  
166 *aeruginosa* (~2000 CFU) or the PBS vehicle was injected into the corneal stroma (Figure  
167 1A), followed by a second injection of 25 µl of either *B. bacteriovorus* strain HD100  
168 ( $4 \times 10^8$  PFU) or the PBS vehicle into the same needle track.

169 The virulent *P. aeruginosa* strain UCBPP-PA14 (PA14) [25-28] was injected into  
170 the cornea at an average of  $1,777 \pm 353$  CFU/cornea. This strain is a clade 2 strain, also  
171 known as a cytotoxic strain, that is ExoU positive and ExoS negative [28]. This strain has  
172 not been previously reported in a rabbit keratitis model to our knowledge. PA14 was able  
173 to replicate 40-fold to  $7.25 \times 10^4$  CFU/cornea by 24 hours (Figure 1B). The eyes were  
174 evaluated with a slit lamp and fluorescein staining using a MacDonald-Shadduck-based

175 scoring system [30] and there was a clear increase in corneal inflammation score by 24  
176 h (Figure 1C-D, 2). This led to corneal perforation in just over half of the infected corneas  
177 (54%) (Figure 1E, 2).

178 By contrast, *B. bacteriovorus* caused intermediate inflammation compared to  
179 PBS and PA14 groups (Figure 1C-E, 2). Moreover, *B. bacteriovorus* injection did not  
180 cause corneal perforations (Figure 1D, 2).

181 *B. bacteriovorus* injected following *P. aeruginosa* correlated with a significant  
182 reduction in *P. aeruginosa* proliferation ( $1.03 \times 10^4$  CFU at 24h,  $p < 0.01$ ) but was still  
183 higher than the inoculum. This reduction did not significantly influence the overall corneal  
184 score, but was associated with a remarkable reduction in the frequency of corneal  
185 perforations (4%,  $p < 0.001$ ) (Figure 1D).

186 Fluorescein staining and slit lamp examination 24 h post-inoculation revealed  
187 minor pathology of the corneas infected with *B. bacteriovorus* that consisted of redness  
188 and a small infiltrate that did not cause a fluorescein stained ulcer (Fig 2). By contrast,  
189 the *P. aeruginosa* injected eyes showed major purulent discharge from the large central  
190 corneal ulcer and anterior chamber effects (Figure 2). Eyes injected with both had an  
191 intermediate phenotype similar to those injected with both the  $\Delta lasR$  *P. aeruginosa* and  
192 predatory bacteria. The eyes injected with just the  $\Delta lasR$  mutant bacteria had minimal  
193 inflammation, though had a corneal ulcer of moderate size (Figure 2).

194 Optical coherence tomography (OCT) was done on a subset of eyes following  
195 sacrifice of the rabbits at 24h post-inject (Figure 3). This reveals the shape of the cornea  
196 and unlike the PBS only injected eye, the *B. bacteriovorus* (HD100) injected eyes had  
197 clear inflammation including an infiltrate and overall edema. The loss of the corneal  
198 integrity was demonstrated in the *P. aeruginosa* PA14 wild-type injected eyes where the  
199 massive infiltrate prevented unobstructed corneal imaging and resulted in shadows. By  
200 contrast, the *P. aeruginosa* wild-type and HD100 coinjected eyes had clear damage,

201 ulceration, and infiltrate, but maintained overall shape. The  $\Delta lasR$  mutant with or without  
202 HD100 had intermediate phenotypes. Movies depicting OCT volumes of corneal layers  
203 are provided in the supplemental information and clearly demonstrate the perforation of  
204 the *P. aeruginosa* strain PA14 infected eye (Supplemental movies S1-3).

205 To evaluate whether infiltrates were made by neutrophils, H&E staining of  
206 corneas was performed. The histology provided consistent results with the fluorescein  
207 staining with respect to maintenance or loss of corneal epithelium (Figure 4). Neutrophils  
208 and severe damage of the anterior stroma were observed in corneas infected by PA14  
209 and to a lesser extent by *B. bacteriovorus* (Figure 4 and Figure S1).

210 Low magnification scanning electron microscopy showed the perforation in the  
211 PA14 infected cornea that was absent in the other corneas (Figure 5). Similar to  
212 fluorescein results (Figure 2), a clear ulcer was evident in corneas infected with PA14  
213 (PA14 + PBS) and *B. bacteriovorus* (PBS + HD100) (Figure 5). At higher power, red and  
214 white blood cells were observed on the ocular surface of most eyes, especially those  
215 infected with PA14 (Figure 5).

216 Consistent with the corneal inflammation MMP9 (92-kDa neutrophil gelatinase or  
217 gelatinase B), an enzyme that digests gelatin and collagen types IV and V [33], and the  
218 pro-inflammatory cytokine interleukin-1 $\beta$  (IL-1 $\beta$ ) were highly induced in corneas infected  
219 with PA14, and to a lesser extend by *B. bacteriovorus* (Figure 6). The co-infection of  
220 PA14 and *B. bacteriovorus* did not significantly alter these pro-inflammatory markers.  
221 However, *B. bacteriovorus* by itself was less inflammatory than PA14 for both MMP9 and  
222 IL-1 $\beta$  ( $p < 0.05$ ).

223

### 224 **3.2. LasR promotes corneal pathogenesis by a cytotoxic *P. aeruginosa* strain.**

225 A recent study showed natural *lasR* mutants at high frequency among bacterial keratitis  
226 isolates [22]. Therefore, the above experiments were also carried out with an isogenic

227 variant of PA14 with a deletion of the *lasR* quorum sensing regulator. This strain was  
228 previously validated by restoring the wild-type allele and is defective in expression of a  
229 number of potential virulence associated phenotypes such as protease production [22].

230         Though slightly more  $\Delta lasR$  mutant bacteria were inoculated compared to the WT  
231 (3,805  $\pm$  1703 CFU/cornea,  $p=0.03$ ), the CFU per cornea at 24 h was significantly lower  
232 at  $5.9 \times 10^3$  CFU/cornea which is 12-fold lower than wild-type PA14,  $p < 0.01$  (Figure 1B).  
233 Corneal inflammation scores were also lower, but did not reach significance ( $p > 0.05$ ),  
234 (Figure 1C). Nevertheless, the  $\Delta lasR$  mutant was defective in causing corneal  
235 perforation compared to the WT (Figure 1D,  $p=0.002$ ). Histology and SEM analysis  
236 demonstrate reduced corneal damage (Figure 2-4), yet the MMP9 and IL-1 $\beta$  levels were  
237 similar to the WT (Figure 6). Both the wild-type PA14 and  $\Delta lasR$  mutant was susceptible  
238 to *B. bacteriovorus* *in vitro*. The mean Log<sub>10</sub> reduction *in vitro* was  $4.9 \pm 0.05$  CFU/ml for  
239 PA14 and  $4.7 \pm 0.15$  CFU/ml for  $\Delta lasR$ ,  $p > 0.05$ ,  $n=3$ . However, the predatory bacteria did  
240 not significantly lower the corneal burden. While corneal scores were high, the frequency  
241 of perforation was low (0%). However, MMP9 and IL-1 $\beta$  were levels in  $\Delta lasR$  and *B.*  
242 *bacteriovorus* inoculate corneas was indistinguishable from PA14 wild-type infected  
243 eyes.

244

#### 245 **4. Discussion**

246 This study demonstrated the severe pathogenesis caused by strain PA14 in a rabbit  
247 corneal infection model. 54% of corneas perforated by 24 h limiting the length of the  
248 study for ethical reasons. While *B. bacteriovorus* on their own caused some  
249 inflammation, they prevented *P. aeruginosa* proliferation and corneal perforation.

250         In this study, MMP9 was strongly induced by *P. aeruginosa*. MMP9 is a  
251 metalloproteinase secreted by neutrophils, macrophages, and corneal epithelial cells  
252 [33]. Transcription of the MMP9 gene was strongly induced when corneal cells are

253 exposed to bacteria [34, 35]. MMP9 is involved in remodeling of the corneal basement  
254 membrane and regulates corneal healing, but has also been linked with corneal  
255 perforation [36, 37]. Tetracyclines inhibit MMP9 activity, and that is one reason that  
256 tetracyclines have been given systemically to patients with corneal ulcers or perforations  
257 [38]. In animal models tetracyclines promoted wound healing and prevented corneal  
258 perforation [39-41]. Our results suggest that MMP9 may contribute to, but is not fully  
259 responsible for corneal perforation caused by *P. aeruginosa* as MMP9 levels remained  
260 in infected corneas that did not perforate. Other factors such as neutrophil elastase,  
261 MMP8, or bacterial proteases such as elastase B, which is positively regulated by LasR  
262 may be key contributors to corneal perforation in our model [42, 43].

263 IL-1 is a major proinflammatory cytokine during bacterial keratitis [44] and  
264 promotes neutrophil mediated corneal damage in mouse models of *P. aeruginosa*  
265 keratitis [45, 46]. Although a role for IL-1 in preventing corneal perforation in young  
266 Swiss mice has also been described [45]. An *in vitro* study showed that keratocytes  
267 produced collagenolytic compounds in an IL-1 dependent manner and that collagen  
268 degradation could be prevented with an IL-1 inhibitor [47]. IL-1 release from damaged  
269 corneal epithelial cells acts as an alarmone and induces increased expression of IL-6  
270 and -8 and reduced barrier function in corneal epithelial cells [48]. Similarly, anti-IL-1 $\beta$   
271 antibody pretreatment reduced MMP9 induction in a mouse (C57Black/6) *P. aeruginosa*  
272 keratitis model leading to the overall model that *P. aeruginosa* induced IL-1 induces the  
273 expression of MMPs resulting in the destruction of corneal tissue [44].

274 In our study, predatory bacteria failed to induce IL-1 $\beta$  production, while this is an  
275 unusual for a Gram-negative bacteria in the corneal stroma, *B. bacteriovorus* have  
276 unusual physiology that may reduce its ability to activate the immune system. Namely, it  
277 has a modified lipopolysaccharide structure that does not activate TLR4 and a  
278 membrane sheathed flagellum, so is unlikely to activate TLR5-mediated inflammation

279 [49, 50]. By contrast, all other infection groups strongly induced IL-1 $\beta$  that correlated with  
280 high levels of MMP9. The intermediate levels of MMP9 induced by *B. bacteriovorus*  
281 suggest that there are IL-1-independent mechanisms to induce MMP9. However, only  
282 one time point was evaluated, so IL-1 may have been induced at early time point by *B.*  
283 *bacteriovorus*. That said, IL-1 induction by bacterial keratitis was reported to be  
284 maintained over the course of several days in a mouse model weakening the likelihood  
285 that IL-1 levels were higher at earlier time points [45]. Although the levels of MMP9  
286 measured in the predator group was significantly lower than that measured in the *P.*  
287 *aeruginosa* infected arm, one should consider that the concentration of the predator  
288 injected was 5 logs higher ( $\sim 4 \times 10^8$  vs  $2 \times 10^3$  respectively). The low inflammatory  
289 stimulating effect of *B. bacteriovorus* seen in this study is in agreement with both *in vitro*  
290 [7, 51, 52] and *in vivo* studies that show that pro inflammatory cytokines, including IL-1,  
291 are not significantly elevated after exposure to the predator [10, 53-56].

292 The role of the LasR quorum sensing marker in *P. aeruginosa* keratitis has  
293 previously been characterized in mouse models using a clade I/invasive/ExoS+ strain  
294 PA01 and similar, but not isogenic *lasR* mutant [57]. Prior work has evaluated the  
295 importance of LasR in *P. aeruginosa* keratitis. These studies both used PA01, an ExoS+  
296 / invasive / clade I strain and a randomly mutated variant of PA01 that was selected for  
297 streptomycin resistance, PA01s with the *lasR* gene replaced by a tetracycline resistance  
298 cassette. The first study demonstrated that in a murine scratch model, 33-fewer *lasR*  
299 mutant bacteria were necessary to establish infections in C3H/HeN mice [58]. The  
300 second study used the same bacterial strains with a murine scratch keratitis model using  
301 BALB/c mice and did not find a difference in the ability of the two bacteria to cause  
302 keratitis, however the *lasR* mutant was not as successful in proliferation with  $\sim 10$ -fold  
303 lower CFU/cornea being measured [59]. Our study, by contrast, used a ExoU+ /  
304 cytotoxic / clade II strain in a rabbit intrastromal injection model. While both the scratch

305 and intrastromal injection models have important limitations, the intrastromal injection  
306 model ensures highly similar inoculation numbers, which are important for a treatment  
307 study, especially when the *lasR* mutant and wild-type express adhesins at different  
308 levels [22]. The results of this study suggest that once past the epithelial barrier the *lasR*  
309 mutant is less able to proliferate and this may account for the highly reduced frequency  
310 of perforations, additionally, the lower expression of collagen digesting proteases such  
311 as elastase B by the *lasR* mutant may also contribute to the highly reduced frequency of  
312 corneal perforations [57, 59]. More work is needed to understand the complex role of  
313 LasR regulated quorum sensing in *P. aeruginosa* keratitis, nevertheless, this study  
314 supports the model that in at least one cytotoxic strain, LasR is required for full levels of  
315 pathogenesis.

316

317 This proof-of-concept study supports that predatory bacteria can prevent bacterial  
318 proliferation and prevent corneal perforation in a keratitis model, however, further study  
319 to test efficacy against established infections by multiple types of *P. aeruginosa* clinical  
320 isolates are necessary to move the concept of using predatory bacteria as a therapeutic  
321 forward.

322

## 323 **5. Acknowledgements**

324 The authors thank Deborah Hogan at Dartmouth Medical School for strains, Kimberly  
325 Brothers and Katherine Davoli for help with animals and histology expertise. This study  
326 was funded by National Institutes of Health grants R01EY027331 (to R.S.) and CORE  
327 Grant P30 EY08098 to the Department of Ophthalmology. The Eye and Ear Foundation  
328 of Pittsburgh and from an unrestricted grant from Research to Prevent Blindness, New  
329 York, NY provided additional departmental funding. This work was also funded by the  
330 U.S. Army Research Office and the Defense Advanced Research Projects Agency

331 (DARPA) and was accomplished under Cooperative Agreement Number W911NF-15-2-  
332 0036 to DEK and RMQS. The views and conclusions contained in this document are  
333 those of the authors and should not be interpreted as representing the official policies,  
334 either expressed or implied, of the Army Research Office, DARPA, or the U.S.  
335 Government. The U.S. Government is authorized to reproduce and distribute reprints for  
336 Government purposes notwithstanding any copyright notation hereon.

337

## 338 **6. Disclosure/Conflict of Interest Statement**

339 The authors have no commercial interests regarding this study.

340

## 341 **7. References**

- 342 [1] Cavallo FM, Jordana L, Friedrich AW, Glasner C, van Dijk JM. *Bdellovibrio*  
343 *bacteriovorus*: a potential 'living antibiotic' to control bacterial pathogens. Crit Rev  
344 Microbiol. 2021;47:630-46.  
345 [2] Atterbury RJ, Tyson J. Predatory bacteria as living antibiotics - where are we now?  
346 Microbiology. 2021;167.  
347 [3] Dharani S, Kim DH, Shanks RMQ, Doi Y, Kadouri DE. Susceptibility of colistin-  
348 resistant pathogens to predatory bacteria. Res Microbiol. 2018;169:52-5.  
349 [4] Negus D, Moore C, Baker M, Raghunathan D, Tyson J, Sockett ER. Predatory versus  
350 pathogen: how does predatory *Bdellovibrio bacteriovorus* interface with the challenges of  
351 killing Gram-negative pathogens in a host setting? Annu Rev Microbiol. 2017;71:441-57.  
352 [5] Kadouri DE, To K, Shanks RM, Doi Y. Predatory bacteria: a potential ally against  
353 multidrug-resistant Gram-negative pathogens. PLoS One. 2013;8:e63397.  
354 [6] Dwidar M, Hong S, Cha M, Jang J, Mitchell RJ. Combined application of bacterial  
355 predation and carbon dioxide aerosols to effectively remove biofilms. Biofouling.  
356 2012;28:671-80.  
357 [7] Shanks RM, Davra VR, Romanowski EG, Brothers KM, Stella NA, Godbole D, et al.  
358 An Eye to a Kill: Using Predatory Bacteria to Control Gram-Negative Pathogens  
359 Associated with Ocular Infections. PLoS One. 2013;8:e66723.  
360 [8] Shanks RM, Kadouri DE. Predatory prokaryotes wage war against eye infections.  
361 Future Microbiol. 2014;9:429-32.  
362 [9] Boileau MJ, Mani R, Breshears MA, Gilmour M, Taylor JD, Clickenbeard KD. Efficacy  
363 of *Bdellovibrio bacteriovorus* 109J for the treatment of dairy calves with experimentally  
364 induced infectious bovine keratoconjunctivitis. Am J Vet Res. 2016;77:1017-28.  
365 [10] Romanowski EG, Stella NA, Brothers KM, Yates KA, Funderburgh ML, Funderburgh  
366 JL, et al. Predatory bacteria are nontoxic to the rabbit ocular surface. Sci Rep.  
367 2016;6:30987.  
368 [11] Cui M, Zheng M, Wiraja C, Chew SWT, Mishra A, Mayandi V, et al. Ocular delivery  
369 of predatory bacteria with cryomicroneedles against eye infection. Adv Sci (Weinh).  
370 2021;8:2102327.

- 371 [12] Romanowski EG, Gupta S, Pericleous A, Kadouri DE, Shanks RMQ. Clearance of  
372 Gram-negative bacterial pathogens from the ocular surface by predatory bacteria.  
373 *Antibiotics (Basel)*. 2021;10:810.
- 374 [13] Fleiszig SMJ, Kroken AR, Nieto V, Grosser MR, Wan SJ, Metruccio MME, et al.  
375 Contact lens-related corneal infection: intrinsic resistance and its compromise. *Prog*  
376 *Retin Eye Res*. 2020;76:100804.
- 377 [14] Miyajima S, Akaike T, Matsumoto K, Okamoto T, Yoshitake J, Hayashida K, et al.  
378 Matrix metalloproteinases induction by pseudomonal virulence factors and inflammatory  
379 cytokines in vitro. *Microb Pathog*. 2001;31:271-81.
- 380 [15] White CD, Alionte LG, Cannon BM, Caballero AR, O'Callaghan RJ, Hobden JA.  
381 Corneal virulence of LasA protease--deficient *Pseudomonas aeruginosa* PAO1. *Cornea*.  
382 2001;20:643-6.
- 383 [16] Hilliam Y, Kaye S, Winstanley C. *Pseudomonas aeruginosa* and microbial keratitis.  
384 *J Med Microbiol*. 2020;69:3-13.
- 385 [17] Vazirani J, Wurity S, Ali MH. Multidrug-Resistant *Pseudomonas aeruginosa*  
386 Keratitis: Risk Factors, Clinical Characteristics, and Outcomes. *Ophthalmology*.  
387 2015;122:2110-4.
- 388 [18] Shen EP, Hsieh YT, Chu HS, Chang SC, Hu FR. Correlation of *Pseudomonas*  
389 *aeruginosa* genotype with antibiotic susceptibility and clinical features of induced central  
390 keratitis. *Invest Ophthalmol Vis Sci*. 2014;56:365-71.
- 391 [19] Green M, Apel A, Stapleton F. Risk factors and causative organisms in microbial  
392 keratitis. *Cornea*. 2008;27:22-7.
- 393 [20] Kadouri DE, Tran A. Measurement of Predation and Biofilm Formation under  
394 Different Ambient Oxygen Conditions Using a Simple Gasbag-Based System. *Appl*  
395 *Environ Microbiol*. 2013;79:5264-71.
- 396 [21] Kadouri D, O'Toole GA. Susceptibility of biofilms to *Bdellovibrio bacteriovorus*  
397 attack. *Appl Environ Microbiol*. 2005;71:4044-51.
- 398 [22] Hammond JH, Hebert WP, Naimie A, Ray K, Van Gelder RD, DiGiandomenico A, et  
399 al. Environmentally Endemic *Pseudomonas aeruginosa* Strains with Mutations in lasR  
400 Are Associated with Increased Disease Severity in Corneal Ulcers. *mSphere*. 2016;1.  
401 [23] Kariminik A, Baseri-Salehi M, Kheirkhah B. *Pseudomonas aeruginosa* quorum  
402 sensing modulates immune responses: An updated review article. *Immunol Lett*.  
403 2017;190:1-6.
- 404 [24] Stolp H, Starr MP. *Bdellovibrio bacteriovorus* Gen. Et Sp. N., A predatory,  
405 ectoparasitic, and bacteriolytic microorganism. *Antonie Van Leeuwenhoek*. 1963;29:217-  
406 48.
- 407 [25] Rahme LG, Stevens EJ, Wolfort SF, Shao J, Tompkins RG, Ausubel FM. Common  
408 virulence factors for bacterial pathogenicity in plants and animals. *Science*.  
409 1995;268:1899-902.
- 410 [26] Finck-Barbancon V, Goranson J, Zhu L, Sawa T, Wiener-Kronish JP, Fleiszig SM, et  
411 al. ExoU expression by *Pseudomonas aeruginosa* correlates with acute cytotoxicity and  
412 epithelial injury. *Mol Microbiol*. 1997;25:547-57.
- 413 [27] Mathee K. Forensic investigation into the origin of *Pseudomonas aeruginosa* PA14 -  
414 old but not lost. *J Med Microbiol*. 2018;67:1019-21.
- 415 [28] Freschi L, Vincent AT, Jeukens J, Emond-Rheault JG, Kukavica-Ibrulj I, Dupont MJ,  
416 et al. The *Pseudomonas aeruginosa* Pan-Genome Provides New Insights on Its  
417 Population Structure, Horizontal Gene Transfer, and Pathogenicity. *Genome Biol Evol*.  
418 2019;11:109-20.
- 419 [29] Hogan DA, Vik A, Kolter R. A *Pseudomonas aeruginosa* quorum-sensing molecule  
420 influences *Candida albicans* morphology. *Mol Microbiol*. 2004;54:1212-23.

- 421 [30] Altmann S, Emanuel A, Toomey M, McIntyre K, Covert J, Dubielzig RR, et al. A  
422 quantitative rabbit model of vaccinia keratitis. Invest Ophthalmol Vis Sci. 2010;51:4531-  
423 40.
- 424 [31] Zhu Z, Waxman S, Wang B, Wallace J, Schmitt SE, Tyler-Kabara E, et al. Interplay  
425 between intraocular and intracranial pressure effects on the optic nerve head in vivo.  
426 Exp Eye Res. 2021;213:108809.
- 427 [32] Schindelin J, Arganda-Carreras I, Frise E, Kaynig V, Longair M, Pietzsch T, et al.  
428 Fiji: an open-source platform for biological-image analysis. Nat Methods. 2012;9:676-82.
- 429 [33] Barletta JP, Angella G, Balch KC, Dimova HG, Stern GA, Moser MT, et al. Inhibition  
430 of pseudomonal ulceration in rabbit corneas by a synthetic matrix metalloproteinase  
431 inhibitor. Invest Ophthalmol Vis Sci. 1996;37:20-8.
- 432 [34] Brothers KM, Harvey SAK, Shanks RMQ. Transcription factor EepR is required for  
433 *Serratia marcescens* host proinflammatory response by corneal epithelial cells.  
434 Antibiotics (Basel). 2021;10:770.
- 435 [35] Chidambaram JD, Kannambath S, Srikanthi P, Shah M, Lalitha P, Elakkiya S, et al.  
436 Persistence of Innate Immune Pathways in Late Stage Human Bacterial and Fungal  
437 Keratitis: Results from a Comparative Transcriptome Analysis. Front Cell Infect  
438 Microbiol. 2017;7:193.
- 439 [36] Fini ME, Parks WC, Rinehart WB, Girard MT, Matsubara M, Cook JR, et al. Role of  
440 matrix metalloproteinases in failure to re-epithelialize after corneal injury. Am J Pathol.  
441 1996;149:1287-302.
- 442 [37] Olivier FJ, Gilger BC, Barrie KP, Kallberg ME, Plummer CE, O'Reilly M, et al.  
443 Proteinases of the cornea and precorneal tear film. Vet Ophthalmol. 2007;10:199-206.
- 444 [38] McElvanney AM. Doxycycline in the management of *Pseudomonas* corneal melting:  
445 two case reports and a review of the literature. Eye Contact Lens. 2003;29:258-61.
- 446 [39] Bian F, Pelegriano FSA, Henriksson JT, Pflugfelder SC, Volpe EA, Li D-Q, et al.  
447 Differential effects of dexamethasone and doxycycline on inflammation and MMP  
448 production in murine alkali-burned corneas associated with dry eye. Ocul Surf.  
449 2016;14:242-54.
- 450 [40] Levy JH, Katz HR. Effect of systemic tetracycline on progression of *Pseudomonas*  
451 *aeruginosa* keratitis in the rabbit. Ann Ophthalmol. 1990;22:179-83.
- 452 [41] Perry HD, Hodes LW, Seedor JA, Donnenfeld ED, McNamara TF, Golub LM. Effect  
453 of doxycycline hydrochloride on corneal epithelial wound healing in the rabbit alkali-burn  
454 model. Preliminary observations. Cornea. 1993;12:379-82.
- 455 [42] Toder DS, Gambello MJ, Iglewski BH. *Pseudomonas aeruginosa* LasA: a second  
456 elastase under the transcriptional control of lasR. Mol Microbiol. 1991;5:2003-10.
- 457 [43] Lin M, Jackson P, Tester AM, Diaconu E, Overall CM, Blalock JE, et al. Matrix  
458 metalloproteinase-8 facilitates neutrophil migration through the corneal stromal matrix by  
459 collagen degradation and production of the chemotactic peptide Pro-Gly-Pro. Am J  
460 Pathol. 2008;173:144-53.
- 461 [44] Xue ML, Wakefield D, Willcox MD, Lloyd AR, Di Girolamo N, Cole N, et al.  
462 Regulation of MMPs and TIMPs by IL-1beta during corneal ulceration and infection.  
463 Invest Ophthalmol Vis Sci. 2003;44:2020-5.
- 464 [45] Rudner XL, Kernacki KA, Hazelett LD. Prolonged elevation of IL-1 in *Pseudomonas*  
465 *aeruginosa* ocular infection regulates microphage-inflammatory protein-2 production,  
466 polymorphonuclear neutrophil persistence, and corneal performance. J Immunol.  
467 2000;164:6576-82.
- 468 [46] Thakur A, Xue M, Stapleton F, Lloyd AR, Wakefield D, Willcox MD. Balance of pro-  
469 and anti-inflammatory cytokines correlates with outcome of acute experimental  
470 *Pseudomonas aeruginosa* keratitis. Infect Immun. 2002;70:2187-97.

- 471 [47] Mishima H, Okamoto J, Nakamura M, Wada Y, Otori T. Collagenolytic activity of  
472 keratocytes cultured in a collagen matrix. *Jap J Ophthalmol.* 1998;42:79-84.
- 473 [48] Fukuda K, Ishida W, Fukushima A, Nishida T. Corneal Fibroblasts as Sentinel Cells  
474 and Local Immune Modulators in Infectious Keratitis. *Int J Mol Sci.* 2017;18.
- 475 [49] Thomashow LS, Rittenberg SC. Isolation and composition of sheathed flagella from  
476 *Bdellovibrio bacteriovorus* 109J. *J Bacteriol.* 1985;163:1047-54.
- 477 [50] Schwudke D, Linscheid M, Strauch E, Appel B, Zahringer U, Moll H, et al. The  
478 obligate predatory *Bdellovibrio bacteriovorus* possesses a neutral lipid A containing  
479 alpha-D-Mannoses that replace phosphate residues: similarities and differences  
480 between the lipid As and the lipopolysaccharides of the wild type strain *B. bacteriovorus*  
481 HD100 and its host-independent derivative HI100. *J Biol Chem.* 2003;278:27502-12.
- 482 [51] Gupta S, Tang C, Tran M, Kadouri DE. Effect of predatory bacteria on human cell  
483 lines. *PLoS ONE.* 2016;11:e0161242.
- 484 [52] Monnappa AK, Bari W, Choi SY, Mitchell RJ. Investigating the responses of human  
485 epithelial cells to predatory bacteria. *Sci Rep.* 2016;15:33485.
- 486 [53] Boileau MJ, Mani R, Breshears MA, Gilmour M, Taylor JD, Clinkenbeard KD.  
487 Efficacy of *Bdellovibrio bacteriovorus* 109J for the treatment of dairy calves with  
488 experimentally induced infectious bovine keratoconjunctivitis. *Am J Vet Res.*  
489 2016;77:1017-28.
- 490 [54] Shatzkes K, Chae R, Tang C, Ramirez GC, Mukherjee S, Tsenova L, et al.  
491 Examining the safety of respiratory and intravenous inoculation of *Bdellovibrio*  
492 *bacteriovorus* and *Micavibrio aeruginosavorus* in a mouse model. *Sci Rep.*  
493 2015;5:12899.
- 494 [55] Shatzkes K, Singleton E, Tang C, Zuena M, Shukla S, Gupta S, et al. Predatory  
495 bacteria attenuate *Klebsiella pneumoniae* burden in rat lungs. *mBio.* 2016;7:e01847-16.
- 496 [56] Shatzkes K, Tang C, Singleton E, Shukla S, Zuena M, Gupta S, et al. Effect of  
497 predatory bacteria on the gut bacterial microbiota in rats. *Sci Rep.* 2017;7:43483.
- 498 [57] Gambello MJ, Iglewski BH. Cloning and characterization of the *Pseudomonas*  
499 *aeruginosa lasR* gene, a transcriptional activator of elastase expression. *J Bacteriol.*  
500 1991;173:3000-9.
- 501 [58] Preston MJ, Seed PC, Toder DS, Iglewski BH, Ohman DE, Gustin JK, et al.  
502 Contribution of proteases and LasR to the virulence of *Pseudomonas aeruginosa* during  
503 corneal infections. *Infect Immun.* 1997;65:3086-90.
- 504 [59] Zhu H, Bandara R, Conibear TC, Thuruthyil SJ, Rice SA, Kjelleberg S, et al.  
505 *Pseudomonas aeruginosa* with *lasI* quorum-sensing deficiency during corneal infection.  
506 *Invest Ophthalmol Vis Sci.* 2004;45:1897-903.
- 507

## 508 8. Figure Legends

509 **Figure 1. Predatory bacteria and *lasR* mutation reduce *P. aeruginosa* pathogenesis in**  
510 **a rabbit keratitis model. A.** Diagram of model in which the rabbit corneal stroma (arrow) is  
511 injected with *P. aeruginosa* strain PA14, isogenic  $\Delta lasR$  mutant, or PBS followed by PBS or  
512 *B. bacteriovorus* strain HD100. **B-D.** Each point represents a rabbit. **a** indicates significant  
513 difference from control group,  $p < 0.05$ . n.s. indicates not significantly different than the control  
514 group. \*\*,  $p < 0.01$ ; \*\*\*,  $p < 0.001$ . **B.** CFU from corneas at 24 h post-injection. Means and SDs

515 are shown. **C.** Corneal inflammation score based on MacDonnald-Shadduck scoring  
516 system. Medians and interquartile ranges are shown and Kruskal-Wallis analysis with  
517 Dunn's post-test was performed. **D.** Corneal perforation frequency. Indicated groups were  
518 compared by Fisher's Exact test.

519

520 **Figure 2. Bright-field microscopy and fluorescein staining of infected eyes.**

521 Representative images are shown. Fluorescein staining indicates corneal ulceration and  
522 loss of corneal epithelium.

523

524 **Figure 3. Optical coherence tomography of infected eyes.** Representative images are  
525 shown. Shadows are due to infiltrates that prevent imaging.

526

527 **Figure 4. Histological analysis demonstrates neutrophil infiltrates.** Representative  
528 images are shown. Magnification was 10X. Polymorphonuclear neutrophils are evident from  
529 inside the stroma and in at the anterior chamber interface.

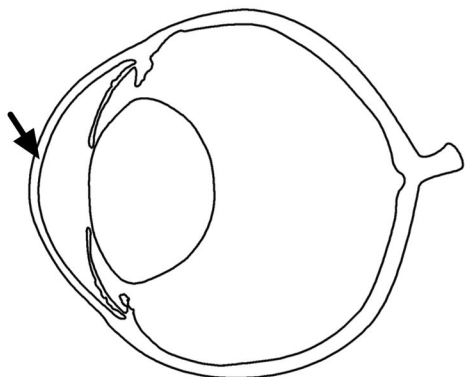
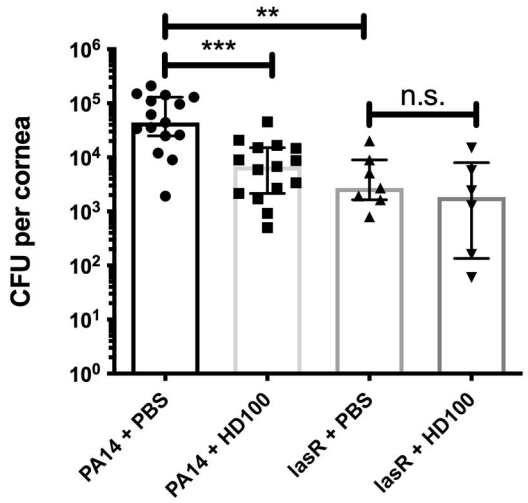
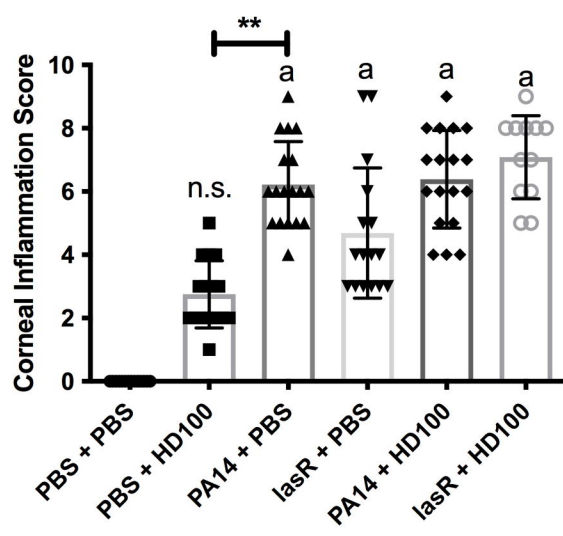
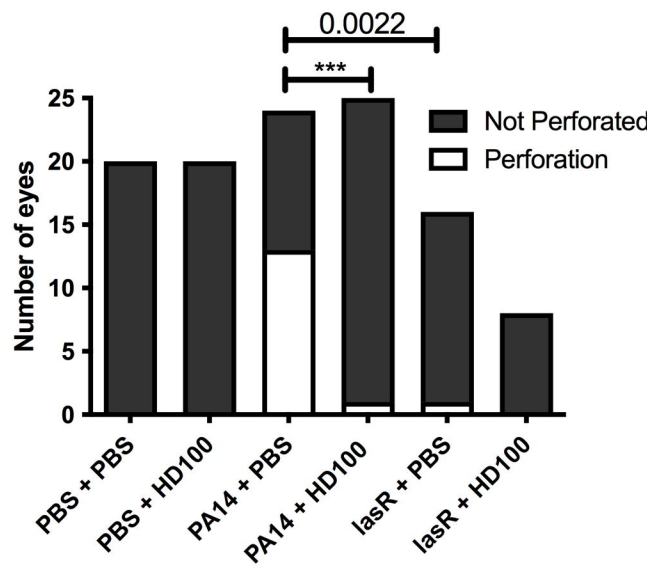
530

531 **Figure 5. Scanning micrographs of rabbit corneal surfaces.** Representative images are  
532 shown. Magnification was 25x (top) and  $\times 500$ x (bottom). The corneal perforation is clearly  
533 shown in the PA14 + PBS injected cornea, and a corneal ulcer was evident in the PA14 with  
534 HD100 injected cornea.

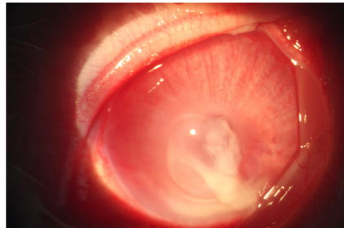
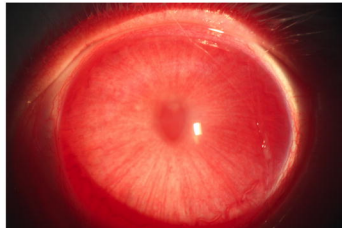
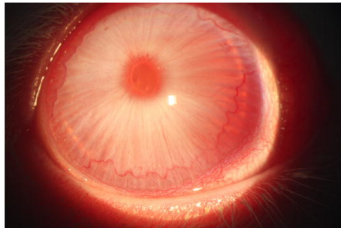
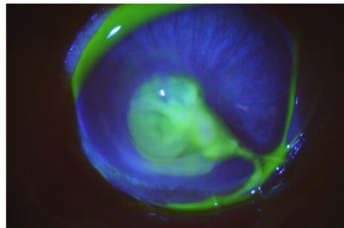
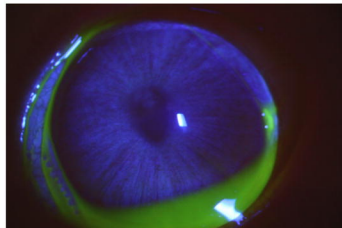
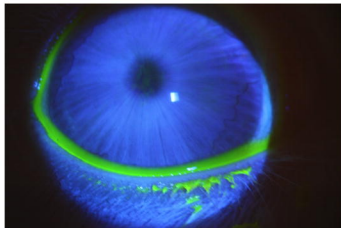
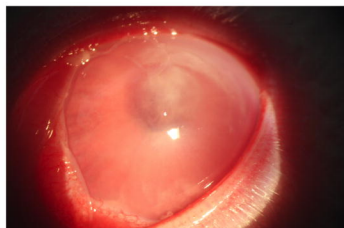
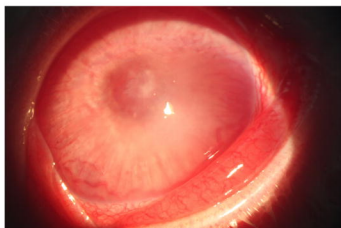
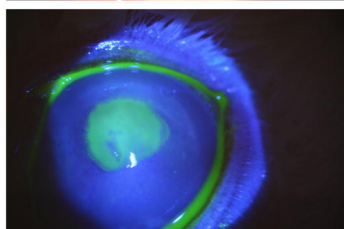
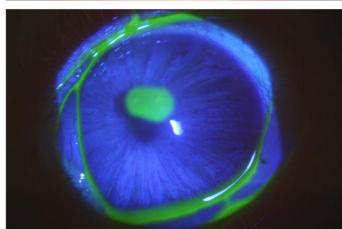
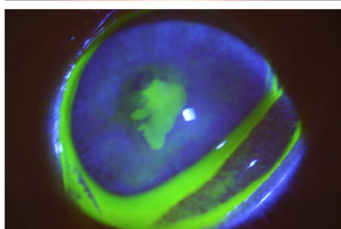
535

536 **Figure 6. *P. aeruginosa* strain PA14 stimulation of gelatinase B (MMP9) and pro-**  
537 **inflammatory cytokine IL-1 $\beta$  from rabbit corneas.** Medians and interquartile ranges of  
538 pro-inflammatory cytokines are shown. Each point represents one rabbit. Kruskal-Wallis with

539     Dunn's post-test was performed, **a** indicates significant difference from control group,  
540      $p < 0.05$ . n.s. indicates not significantly different than the control group. \*,  $p < 0.05$ ; \*\*,  $p < 0.01$ .

**A****B****C****D**

**Figure 1. Predatory bacteria and *lasR* mutation reduce *P. aeruginosa* pathogenesis in a rabbit keratitis model.** **A.** Diagram of model in which the rabbit corneal stroma (arrow) is injected with *P. aeruginosa* strain PA14, isogenic  $\Delta$ *lasR* mutant, or PBS followed by PBS or *B. bacteriovorus* strain HD100. **B-D.** Each point represents a rabbit. a indicates significant difference from control group,  $p < 0.05$ . n.s. indicates not significantly different than the control group. \*\*,  $p < 0.01$ ; \*\*\*,  $p < 0.001$ . **B.** CFU from corneas at 24 h post-injection. Means and SDs are shown. **C.** Corneal inflammation score based on MacDonnald-Shadduck scoring system. Medians and interquartile ranges are shown and Kruskal-Wallis analysis with Dunn's post-test was performed. **D.** Corneal perforation frequency. Indicated groups were compared by Fisher's Exact test.

**PBS + PBS****PBS + HD100****PA14 + PBS****bright-field****fluorescein****PA14 + HD100*****lasR* + PBS*****lasR* + HD100****bright-field****fluorescein**

**Figure 2. Bright-field microscopy and fluorescein staining of infected eyes.** Representative images are shown. Fluorescein staining indicates corneal ulceration and loss of corneal epithelium.

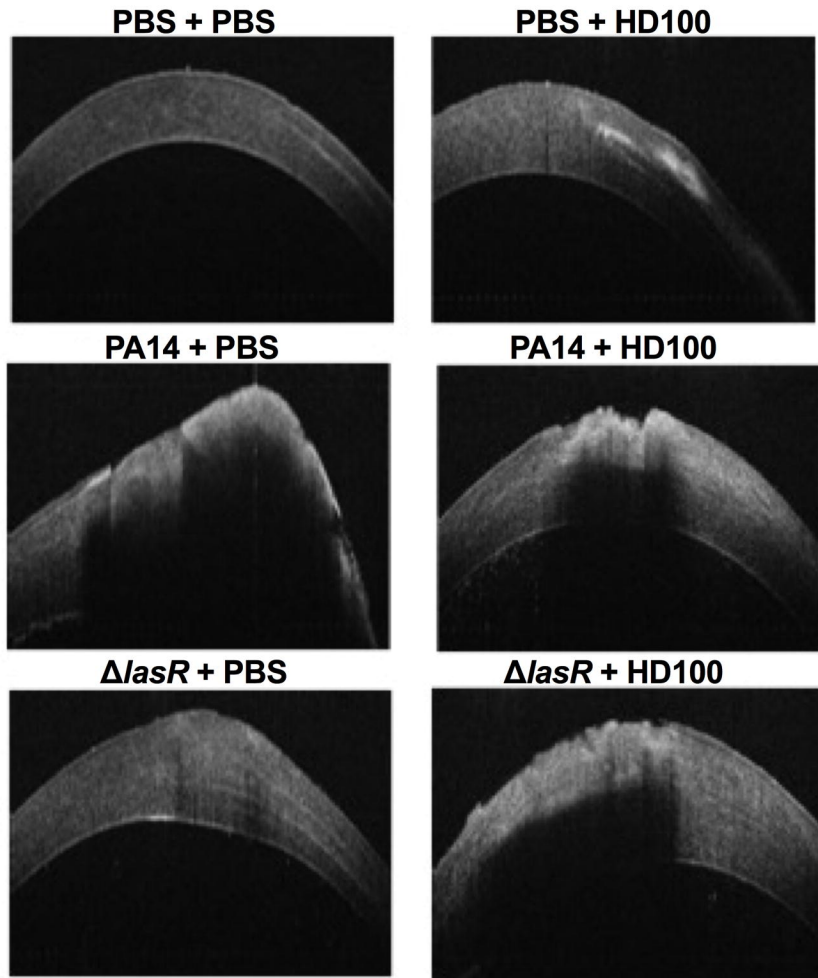


**Figure 3. Optical coherence tomography of infected eyes.** Representative images are shown. Shadows are due to infiltrates that prevent imaging.

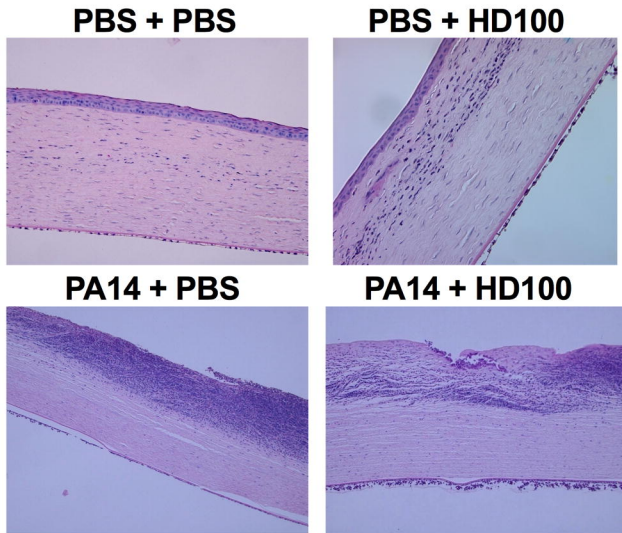


**Figure 4. Histological analysis demonstrates neutrophil infiltrates.** Representative images are shown. Magnification was 10X. Polymorphonuclear neutrophils are evident from inside the stroma and in at the anterior chamber interface.

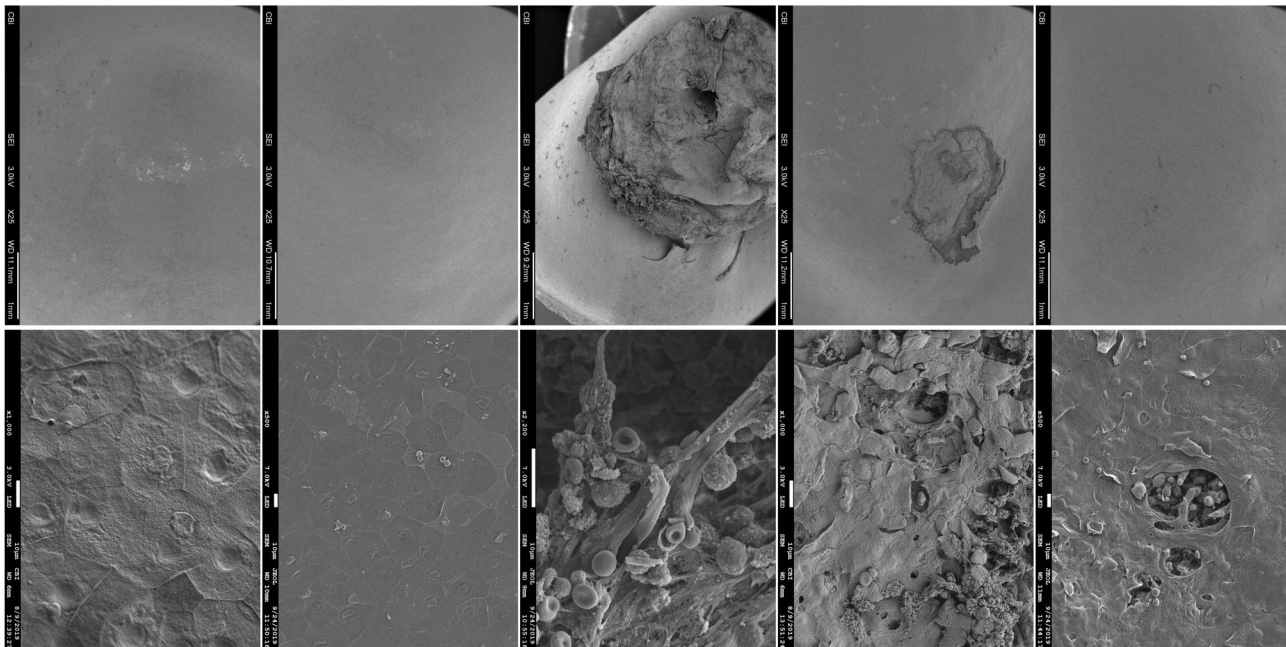
25X

PBS + PBS

PBS + HD100

PA14 + PBS

PA14 + HD100

 $\Delta lasR$  + PBS

≥500X

**Figure 5. Scanning micrographs of rabbit corneal surfaces.** Representative images are shown. Magnification was 25x (top) and ≥500x (bottom). The corneal perforation is clearly shown in the PA14 + PBS injected cornea, and a corneal ulcer was evident in the PA14 with HD100 injected cornea.

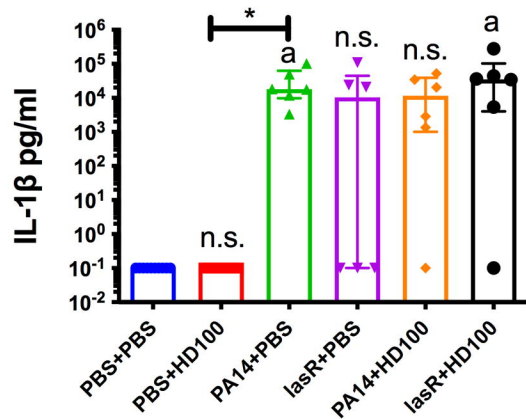
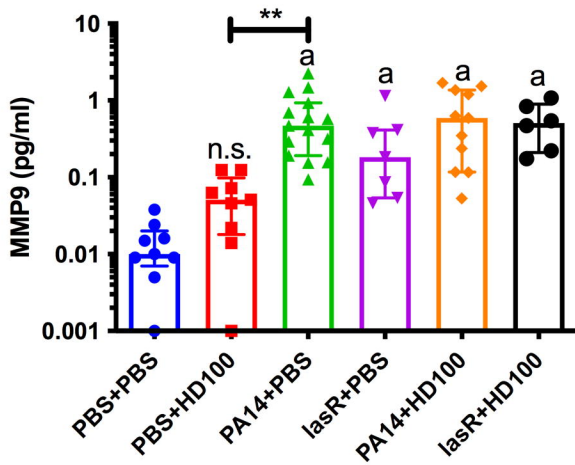


**Figure 6. *P. aeruginosa* strain PA14 stimulation of gelatinase B (MMP9) and pro-inflammatory cytokine IL-1 $\beta$  from rabbit corneas.** Medians and interquartile ranges of pro-inflammatory cytokines are shown. Each point represents one rabbit. Kruskal-Wallis with Dunn's post-test was performed, **a** indicates significant difference from control group,  $p < 0.05$ . n.s. indicates not significantly different than the control group. \*,  $p < 0.05$ ; \*\*,  $p < 0.01$ .